Journal of Statistical Physics, Vol. 52, Nos. 3/4, 1988

Immiscible Cellular-Automaton Fluids

Daniel H. Rothman[1] **and Jeffrey M. Keller**[1]

Received April 7, 1988

We introduce a new deterministic collision rule for lattice-gas (cellular-automaton) hydrodynamics that yields immiscible two-phase flow. The rule is based on a minimization principle and the conservation of mass, momentum, and particle type. A numerical example demonstrates the spontaneous separation of two phases in two dimensions. Numerical studies show that the surface tension coefficient obeys Laplace's formula.

KEY WORDS: Cellular automata; lattice gases; surface tension; phase separation; two-phase flow.

Recently, Frisch *et al.*[1] (FHP) introduced a discrete lattice-gas model for the numerical solution of the 2D incompressible Navier-Stokes equations. In their model, space, time, and the velocities of particles are discrete. Identical particles of equal mass populate a triangular lattice, obey simple collision rules, and travel to neighboring sites at each time step. Because the model is entirely discrete, and because the evolution of a site is determined by the state of the site and its nearest neighbors, the lattice gas is a cellular automaton.[2] Despite its simplicity, the macroscopic behavior of the lattice-gas automaton asymptotically approaches continuum flow. Since its introduction, this new model of fluid dynamics has not only been the subject of extensive theoretical and numerical studies,[3–7] but has also been extended to 3D[8] and applied to a wide range of problems (e.g., refs. 9–11).

Here we introduce a simple yet fundamental extension of the lattice gas that leads to immiscible two-phase flow with interfacial tension between fluid phases. In regions occupied by only a single phase, our 2D model is (barring irrelevant details) identical to the FHP gas. When two phases occupy the same region, however, we apply a new collision rule that

[1] Department of Earth, Atmospheric, and Planetary Sciences, Massachusetts Institute of Technology, Cambridge, Massachusetts 02139.

0022-4715/88/0800-1119$06.00/0

causes preferential grouping of like phases. To demonstrate the validity of our model, we provide empirical evidence that it correctly honors the physics of interfacial tension. Of course, the asymptotic arguments of FHP apply equally well to our model in regions of homogeneity.

The equations of motion for immiscible two-phase flow are given by the Navier–Stokes equations within each phase, and by boundary conditions at the interfaces between phases.[12,13] The incompressible Navier–Stokes equations are

$$\nabla \cdot \mathbf{u} = 0 \tag{1}$$

$$\rho\, \partial_t \mathbf{u} + \rho(\mathbf{u} \cdot \nabla)\, \mathbf{u} = -\nabla p + \mu\, \nabla^2 \mathbf{u} \tag{2}$$

where ρ denotes the density, $\mathbf{u}$ the velocity, p the pressure, and μ the shear viscosity. Two boundary conditions govern the behavior of an interface. The first is the purely kinematical statement that the component of velocity locally normal to the boundary in each phase must equal the normal component of the interfacial velocity:

$$\mathbf{u}_1 \cdot \mathbf{n} = \mathbf{u}_2 \cdot \mathbf{n} = \mathbf{u}_{\text{int}} \cdot \mathbf{n} \tag{3}$$

Here the subscripted velocities refer to the two phases and the interface; $\mathbf{n}$ is the unit normal to the interface. The second boundary condition is a dynamical description of the momentum flux across the interface. The requirement here is that the stress difference at the interface be balanced by surface tension. In 2D, this equation is

$$\mathbf{T}_2 \cdot \mathbf{n} - \mathbf{T}_1 \cdot \mathbf{n} = (\sigma/R)\, \mathbf{n} \tag{4}$$

where σ is the surface tension coefficient, R is the radius of curvature (considered positive when the center of curvature is on side one), and $\mathbf{T}_1$ and $\mathbf{T}_2$ denote the stress tensor $\mathbf{T} = -p\mathbf{I} + \mu[\nabla \mathbf{u} + (\nabla \mathbf{u})^T]$ in phases 1 and 2, respectively.

Of these four equations, the FHP gas, after a rescaling of variables and macroscopic averaging, models the first two. The idea of FHP is to set up a triangular lattice, with identical particles traveling between neighboring sites at each time step. Up to six particles, each with unit velocity, may reside at a site, but there may be at most one particle moving in each of the six possible directions. When particles meet at the same site, they obey collision rules that conserve mass (particle number) and momentum. Macroscopic fields are obtained by coarse-grain averaging in space and time; the correspondence of these macroscopic fields to Eq. (1) and (2) is primarily due to the microscopic conservation of mass and momentum and the symmetries of the triangular lattice.

To model two-phase flow, one must satisfy not only Eq. (1) and (2), but also the boundary conditions (3) and (4). Our two-phase model is built upon the FHP foundation. We define two kinds of particles, and refer to them by *color*, "red" and "blue."[7,9] In addition to conserving mass and momentum, however, collisions must now also conserve the number of reds (or blues) and encourage the preferential grouping of like colors.

We employ a version of the FHP model that includes zero-velocity "rest particles"[1,3,6]; there are thus seven available velocities. The ith velocity vector is denoted by $\mathbf{c}_i$; $\mathbf{c}_0 = 0$ and $\mathbf{c}_1$ through $\mathbf{c}_6$ are unit vectors connecting neighboring sites on the triangular lattice. Red and blue particles may simultaneously occupy the same site, but not with the same velocity. The Boolean variable $r_i(\mathbf{x}) \in \{0, 1\}$ indicates the presence or absence of a red particle with velocity $\mathbf{c}_i$ at lattice site $\mathbf{x}$; the variable $b_i(\mathbf{x}) \in \{0, 1\}$ plays the same role for a blue particle. The configuration at a site is thus completely described by the two seven-bit variables $r = \{r_i, i = 0,..., 6\}$ and $b = \{b_i, i = 0,..., 6\}$. Note that b_i and r_i cannot both equal one.

Cohesion in real liquids results from short-range intermolecular forces of attraction.[14] We model these short-range forces by allowing the particles at sites which are the nearest neighbors of site $\mathbf{x}$ to influence the configuration of particles at site $\mathbf{x}$. Specifically, we define a local *color flux* and a local *color field*, and design collision rules such that the "work" performed by the flux against the field is minimized, subject to the constraints of mass, momentum, and color conservation.

The local color flux $\mathbf{q}[r(\mathbf{x}), b(\mathbf{x})]$ is defined to be the difference between the net red momentum and net blue momentum at site $\mathbf{x}$:

$$\mathbf{q}[r(\mathbf{x}), b(\mathbf{x})] \equiv \sum_i \mathbf{c}_i [r_i(\mathbf{x}) - b_i(\mathbf{x})] \tag{5}$$

The local color field $\mathbf{f}(\mathbf{x})$ is defined to be the direction-weighted sum of the differences between the number of reds and the number of blues at neighboring sites [i.e., the microscopic gradient of the signed (red minus blue) color density]:

$$\mathbf{f}(\mathbf{x}) \equiv \sum_i \mathbf{c}_i \sum_j [r_j(\mathbf{x} + \mathbf{c}_i) - b_j(\mathbf{x} + \mathbf{c}_i)] \tag{6}$$

The work W performed by the flux against the field is then

$$W(r, b) = -\mathbf{f} \cdot \mathbf{q}(r, b) \tag{7}$$

Here we have incorporated repulsive forces between different colors in

addition to attractive forces between like colors. The result of a collision, $r \to r'$, $b \to b'$, is determined by the solution to the mimimization problem

$$W(r', b') = \min_{r'', b''} W(r'', b'') \tag{8}$$

subject to the constraints of colored mass conservation

$$\sum_i r_i'' = \sum_i r_i, \qquad \sum_i b_i'' = \sum_i b_i \tag{9}$$

and colorblind momentum conservation

$$\sum_i \mathbf{c}_i(r_i'' + b_i'') = \sum_i \mathbf{c}_i(r_i + b_i) \tag{10}$$

If the solution is nonunique, the outcome of a collision is chosen with equal *a priori* weight from the set of configurations that satisfy (8)–(10). In the resulting configuration, particles of each color will be preferentially moving toward concentrations of like color and away from concentrations of unlike color. Once collisions have occurred, each particle moves one lattice unit in its direction of motion.

In our implementation, the collision rules determined by Eq. (5)–(10) are stored in a table. Because the number of unique configurations at a site and its six nearest neighbors is large, $(3^7)^7$, we reduce the size of the table by noting that the magnitude of a nonzero color field $\mathbf{f}$ does not affect the minimization in Eq. (8). Thus, we need only specify a unit vector $\hat{\mathbf{f}}$; in practice, we allow only $N = 36$ discrete values $\hat{\mathbf{f}}_k = (\cos(2\pi k/N), \sin(2\pi k/N))$, $k = 1,..., N$. The input to the table then consists of an integer representing the conserved quantities in Eq. (9) and (10) in addition to the number k. Our implementation has been coded in C and runs at approximately 12,000 site updates per second on a Sun 3/160 workstation.

Figure 1 illustrates the nonequilibrium behavior of the two-fluid automaton. The initial configuration is a random mixture. The reduced density is $d = \rho/7 = 0.75$; ρ is the average number of particles per site. There are 128^2 sites; boundaries are periodic, both horizontally and vertically. The initial distribution of particles is random, with reds and blues equally probable. In the plots, a site is black if the number of blue particles at that site is greater than or equal to the number of red particles; otherwise, it is gray. No averaging has been performed.

The automaton quickly acts to smooth out all surfaces, producing a number of 2D bubbles. Random motion eventually causes small bubbles to meet, producing even larger bubbles. The final equilibrium state is full separation, with plane horizontal interfaces.

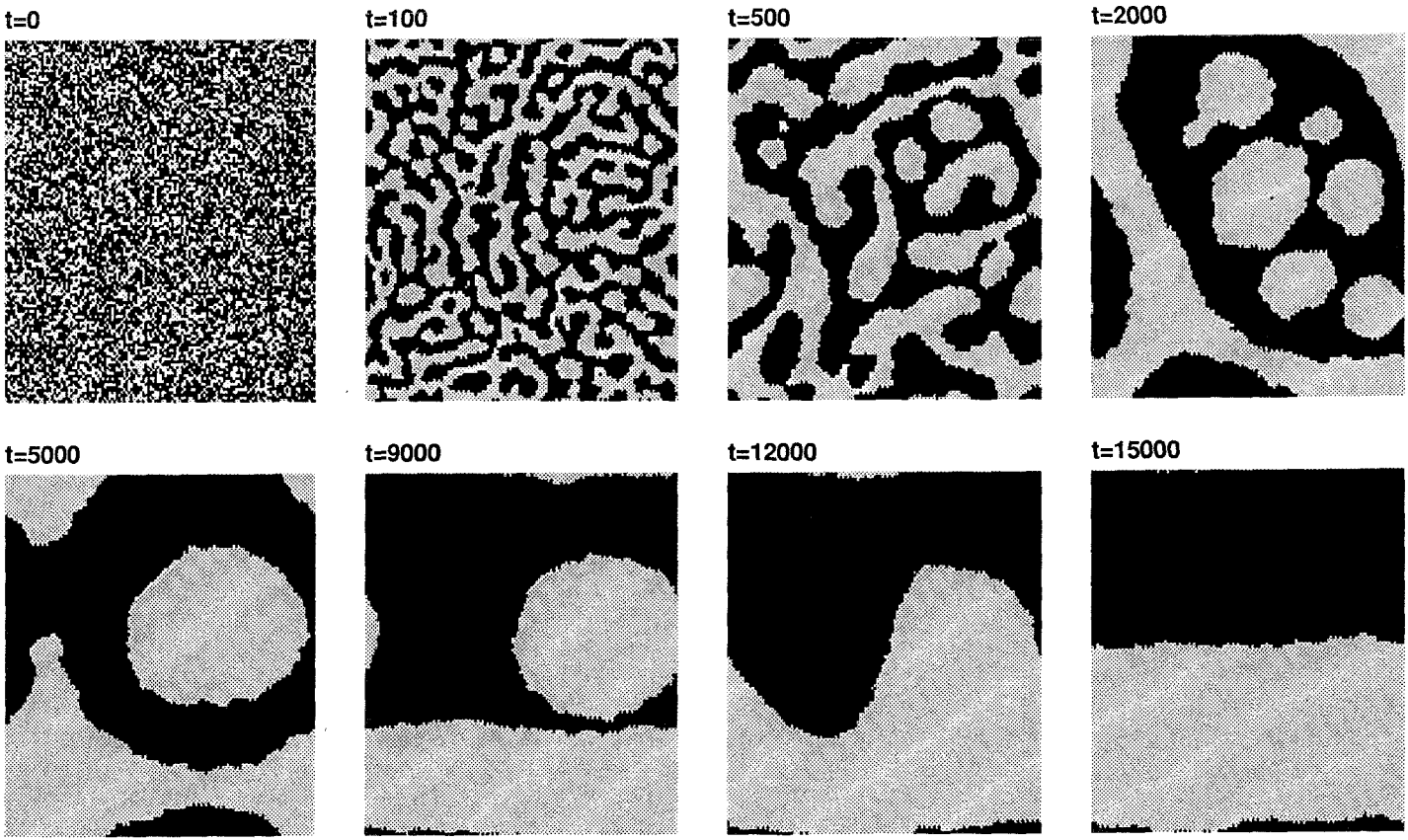

Fig. 1. Nonequilibrium behavior of the two-phase automaton, illustrated at representative time steps. The initial configuration is a random mixture.

Quantitative tests show that the automaton is indeed modeling surface tension. We test the validity of Eq. (4) for the simplified case of no flow. This boundary condition is then Laplace's formula,[13]

$$p_1 - p_2 = \sigma/R \tag{11}$$

Figure 2 is a plot of $\Delta p = p_1 - p_2$ versus $1/R$, where R is the radius of a 2D bubble. Pressure is calculated from the equation of state $p = 3\rho/7$ given in ref. 3. The tests were performed by initializing a lattice of size $(4R)^2$ with a blue bubble of radius R in a sea of red, with $d = 0.70$ and $\mathbf{u} = 0$ in both phases. The bubble maintains its gross shape; Δp is measured by computing the difference between the average density of sites occupied by only blue particles and the average density of sites occupied by only red particles.[2] R varies from 16 to 48; the resulting density contrast ranges from about 0.03 to 0.01 particle per site. As with real bubbles, these 2D bubbles undergo free oscillations evident in plots of Δp versus time. Here we have simply averaged Δp over 2000 time steps beginning at time step 500. For each R, this calculation is performed four times with different initial configurations. The graph shows the mean and standard deviation of the

[2] Empty sites and mixed sites containing both red and blue particles are not counted in the estimation of the density difference. The discounting of empty sites results in a negligible error smaller than $(1-d)^7 \approx 2.2 \times 10^{-4}$ times the true density difference. Observations show that mixed sites virtually always occur on the perimeter of the bubble; indeed, in the example of Fig. 1 an average of only 2–3 mixed sites may be found away from the interfaces at any one time after 100 time steps. Measurements made in the bubble tests show that the number of mixed sites is approximately $1.3 \times 2\pi R$.

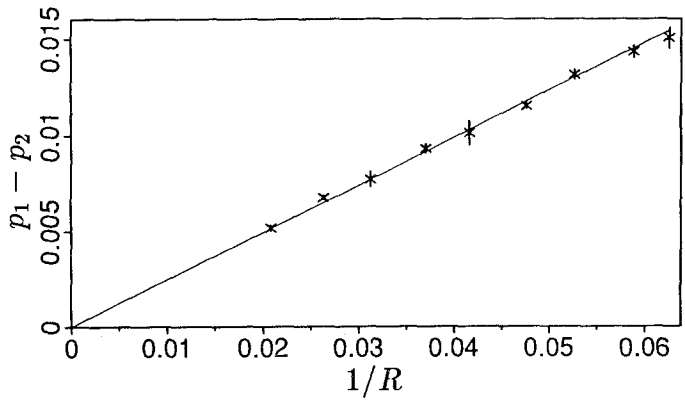

Fig. 2. Numerical confirmation of Laplace's formula, Eq. (11). R is the radius of a 2D bubble. The surface tension is given by the slope of the straight line.

averages computed in the four runs, for each value of R, compared to the best-fitting line through the origin. As predicted by Eq. (11), Δp is proportional to $1/R$; the slope $\sigma = 0.246 \pm 0.002$ is the surface tension.

Figure 3 depicts the continuous variation of surface tension with density. Surface tension is low at low densities, primarily because fewer particles provide fewer choices in the minimization of W. At unusually high densities the surface tension is also low, but surfaces do not break; σ vanishes at $d = 1$ because Δp is necessarily zero at maximum density. Surface tension also vanishes for $d \leqslant 0.4$, the low densities typical of most lattice-gas computations. However, because our single-color model is invariant under duality (exchange of particles and holes), the hydrodynamics of single-color simulations at densities d and $1-d$ are equivalent.[3]

We emphasize that in regions of only one color, our model is precisely model III of ref. 6 with the exception that the possible outcomes of a collision in our model include the precollision state. The only consequence of this difference is an increase in viscosity; the model's adherence to the Navier-Stokes equations is unchanged. A theoretical prediction of the Laplace law, however, remains an outstanding problem. One promising approach might be to use the mechanical definition of surface tension, $\sigma = \int_{-\infty}^{\infty} [p - p_T(z)]\, dz$, where p is the component of the pressure tensor normal to the interface (in the x, y plane) and p_T is the transverse component.[14] A theoretical expression for p_T might be obtainable from lattice-gas theory,[1,3,4] but it is made complicated here by our unusual collision rules.

Of the two boundary conditions, we have quantitatively studied only Eq. (4). Because we have observed the continuous flow of surfaces without

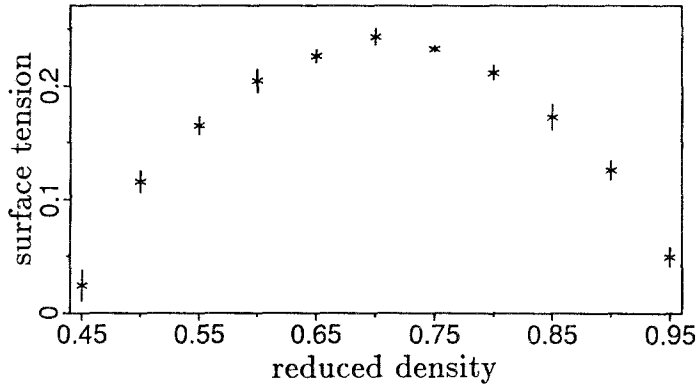

Fig. 3. Numerical measurements of surface tension as a function of reduced density.

rupture, we take the automaton's adherence to Eq. (3) to be self-evident for **u** measured from the lattice. However, the momentum equation (2) is formally attained only after a rescaling of variables to attain Galilean invariance[1,3]; this rescaling does not apply to the velocity of the interface. Thus, our model as it stands lacks Galilean invariance. d'Humières *et al.*[7] have shown, however, that the FHP collision rules can be tuned to provide Galilean invariance without a rescaling of variables; their corrections should be applicable to our model as well.

We comment briefly on extensions of the model. Fluids of different viscosities may be modeled by either limiting the set of possible collisions in one fluid or by decreasing the frequency of collisions in one fluid. Buoyant forces may be modeled using the techniques described in ref. 9. Extensions to 3D[8] are straightforward in principle. Flow of three or more fluids can be modeled by dispensing with the unified expressions for the flux and field given by Eq. (5) and (6), and instead defining red fields, blue fields, and, say, green fields, and likewise for the fluxes. The (possibly weighted) sum of the work of each flux against the corresponding field of the same color would then be minimized. No repulsive forces would be modeled, but we do not consider them necessary.

We have presented a new model, based on discrete dynamics, for the solution of the flow equations for two immiscible fluids. Surface tension and phase separation, two fundamental phenomena of immiscible fluid mixtures, have been demonstrated to arise from the model. Applications to problems in two-phase flow should now be straightforward. In particular, we expect that the model will be useful for the study of a variety of two-fluid instability phenomena, possibly with increased versatility and efficiency over other methods.[15] The simplicity of this automaton for two-phase flow should thus provide not only a novel approach to the study of fluid mixtures, but also possibly the ability to study computationally what has heretofore been accessible only be experiment.

ACKNOWLEDGMENTS

It is a pleasure to thank Stéphane Zaleski for numerous thought-provoking discussions. We also thank A. Gunstensen for technical assistance, J. Berryman, B. Boghosian, and T. Madden for their advice and encouragement, and S. Cole, J. Dellinger, and R. Ottolini of the Stanford Exploration Project for providing graphics software. This work was supported in part by Army Research Office grant DAAG29-85-K-0226, the donors of the Petroleum Research Fund, administered by the American Chemical Society, and by the Department of Earth, Atmospheric, and Planetary Sciences, MIT.

REFERENCES

1. U. Frisch, B. Hasslacher, and Y. Pomeau, *Phys. Rev. Lett.* **56**:1505 (1986).
2. S. Wolfram, *Theory and Applications of Cellular Automata* (World Scientific, Singapore, 1986).
3. U. Frisch, D. d'Humières, B. Hasslacher, P. Lallemand, Y. Pomeau, and J.-P. Rivet, *Complex Systems* **1**:648 (1987).
4. S. Wolfram, *J. Stat. Phys.* **45**:471 (1986).
5. L. Kadanoff, G. McNamara, and G. Zanetti. From automata to fluid flow: comparisons of simulation and theory, University of Chicago preprint (1987).
6. D. d'Humières and P. Lallemand, *Complex Systems* **1**:598 (1987).
7. D. d'Humières, P. Lallemand, and G. Searby, *Complex Systems* **1**:632 (1987).
8. D. d'Humières, P. Lallemand, and U. Frisch, *Europhys. Lett.* **2**:291 (1986); J.-P. Rivet, *C. R. Acad. Sci. Paris II* **305**:751 (1987).
9. C. Burges and S. Zaleski, *Complex Systems* **1**:31 (1987).
10. K. Balasubramanian, F. Hayot, and W. F. Saam, *Phys. Rev. A* **36**:2248 (1987).
11. D. Rothman, *Geophysics* **53**:509 (1988).
12. D. A. Drew, *Annu. Rev. Fluid Mech.* **15**:261 (1983).
13. L. D. Landau and E. M. Lifshitz, *Fluid Mechanics* (Pergamon Press, New York, 1959), p. 230; G. K. Batchelor, *An Introduction to Fluid Dynamics* (Cambridge University Press, Cambridge, 1976), p. 68.
14. J. S. Rowlinson and B. Widom, *Molecular Theory of Capillarity* (Clarendon Press, Oxford, 1982).
15. J. M. Hyman, *Physica* **12D**:396 (1984), and references therein; J. Glimm, O. McBryan, R. Menikoff, and D. H. Sharp, *SIAM J. Sci Stat. Comput.* **7**:230 (1986); H. Aref, Finger, bubble, tendril, spike, University of California-San Diego preprint (1987).

Communicated by J. L. Lebowitz